



Contents lists available at ScienceDirect

## Nuclear Instruments and Methods in Physics Research B

journal homepage: [www.elsevier.com/locate/nimb](http://www.elsevier.com/locate/nimb)

# A critical study on electronic processes involving electron capture and ionization of He targets by interaction with multiply charged ion beams

P.N. Terekhin<sup>a,b,\*</sup>, P.R. Montenegro<sup>a</sup>, M.A. Quinto<sup>a</sup>, J.M. Monti<sup>a,c</sup>, O.A. Fojón<sup>a,c</sup>, R.D. Rivarola<sup>a,c</sup>

<sup>a</sup> Instituto de Física Rosario (CONICET-UNR), Bv 27 de Febrero, 2000 Rosario, Argentina

<sup>b</sup> National Research Centre 'Kurchatov Institute', Kurchatov Sq. 1, 123182 Moscow, Russia

<sup>c</sup> Laboratorio de Colisiones Atómicas, Facultad de Ciencias Exactas, Ingeniería y Agrimensura, Universidad Nacional de Rosario, Av. Pellegrini 250, 2000 Rosario, Argentina

## ARTICLE INFO

## Article history:

Received 29 November 2016

Received in revised form 6 March 2017

Accepted 25 March 2017

Available online xxx

## Keywords:

Electron ionization

Electron capture

Transfer-ionization

Highly charged ions

## ABSTRACT

The interest of the present work is focused on theoretical calculations of single electron ionization, single electron capture and transfer-ionization reactions of He targets interacting with bare ion beams. In order to investigate all these processes, the corresponding transition probabilities are determined in the framework of the prior-version of the three-body Continuum Distorted Wave-Eikonal Initial State model (3B-CDW-EIS). A theoretical description using a trinomial probability analysis based on 3B-CDW-EIS is also presented to analyze its limitations for the studied reactions. The cases of He<sup>2+</sup> and Li<sup>3+</sup> projectiles are considered at intermediate and high collision energies. A unitarization procedure is employed to avoid transition probabilities larger than one at intermediate velocities.

© 2017 Elsevier B.V. All rights reserved.

## 1. Introduction

Dynamical interaction of bare ion projectiles impacting on He atoms is the simplest multi-electronic system to investigate electron transitions. The study of these collisional systems is crucial to fully understand the mechanisms underlying these basic reactions. Moreover, they are of interest in several fields such as astrophysics [1], thermonuclear fusion [2] and hot plasmas [3], among other areas.

In the early days, experimental data for electronic reactions were provided mainly measuring projectile or target ion charges in the exit channel, combining them in some cases with the resulting radiation emission. Moreover, the corresponding cross sections were usually normalized to other theoretical and experimental predictions. Nowadays, using cold target recoil ion momentum spectroscopy (COLTRIMS) techniques, kinematically complete experiments are feasible [4], allowing to investigate separately different electronic reactions, such as single ionization, single capture and transfer-ionization. Thus, these new facilities open the possibility to test new theoretical descriptions in the same way as experiments were done, for a more appropriate comparison between them and for a better understanding of the different electron transition processes studied.

The aim of this work is to present single electron ionization (SI), single electron capture (SC) and two-electron-transfer-ionization (TI) cross sections of He targets impacted by He<sup>2+</sup> and Li<sup>3+</sup> projectiles at intermediate and high collision energies. They are computed through the determination of transition probabilities as a function of the impact parameter in the framework of the 3B-CDW-EIS model. A unitarization procedure appears as necessary to avoid overestimations of 3B-CDW-EIS impact parameter probabilities. Two different models are employed, 3B-CDW-EIS developed by Rivarola and co-workers for single-electron capture [5] as well as for single electron ionization [6], and another one, where a trinomial probability analysis (TPA) based on 3B-CDW-EIS ones are used [7,8]. Both approximations are calculated in order to discern their adequacy to describe the different electronic reactions. It must be mentioned that an approximation employing binomial probabilities has been previously applied with some success to describe multiple electron ionization of atomic and molecular targets at high impact energies [9–11].

Unless otherwise stated, atomic units ( $m_e = \hbar = e = 1$ ) will be used.

## 2. Theory

The 3B-CDW-EIS model is employed to calculate the transition probabilities for both single electron ionization [12] and single electron capture [13,14]. Originally, Crothers and McCann developed this model [15] for SI of hydrogenic targets and later on it

\* Corresponding author at: Instituto de Física Rosario (CONICET-UNR), Bv 27 de Febrero, 2000 Rosario, Argentina.

E-mail address: [P.N.Terekhin@yandex.ru](mailto:P.N.Terekhin@yandex.ru) (P.N. Terekhin).

was extended [6] with great success for multielectronic targets, assuming that except for the active electron all the residual ones remain as frozen in their initial orbitals. This is a key point in our analysis. Within the straight-line version of the impact parameter approximation ( $\mathbf{R} = \boldsymbol{\rho} + \mathbf{v}t$ , with  $\mathbf{R}$  being the internuclear vector,  $\boldsymbol{\rho}$  the impact parameter,  $\mathbf{v}$  the collision velocity and  $t$  the evolution time) this formulation was based on a deduction previously obtained for SC [5] and which has a general character, independently of the theoretical model employed. Thus, for SI or SC the problem was reduced to find scattering solutions of a one-active electron Hamiltonian

$$H = -\nabla^2/2 - Z_T/x - Z_P/s + V_{ap}(\mathbf{x}) + V_S(\mathbf{R}), \quad (1)$$

where  $Z_T$  and  $Z_P$  are the target and projectile nucleus charges,  $\mathbf{x}$  and  $\mathbf{s}$  represent the position vectors of the active electron with respect to the target and projectile, respectively, and,

$$V_{ap}(\mathbf{x}) = \left\langle \varphi_p(\{\mathbf{x}_{p i}\}) \left| \sum_{i=1}^{N_p} \frac{1}{|\mathbf{x} - \mathbf{x}_{p i}|} \right| \varphi_p(\{\mathbf{x}_{p i}\}) \right\rangle \quad (2)$$

is a potential that takes into account the interaction of the active electron with the passive ones, being  $\varphi_p(\{\mathbf{x}_{p i}\})$  the wavefunction corresponding to the  $N_p$  passive electrons and  $\mathbf{x}_{p i}$  is the ensemble of position vectors of the  $i$ th passive electrons with respect to the target nucleus. Also in Eq. (2),  $V_S(\mathbf{R})$  is the static potential

$$V_S(\mathbf{R}) = \frac{Z_P Z_T}{R} + \left\langle \varphi_p(\{\mathbf{x}_{p i}\}) \left| - \sum_{i=1}^{N_p} \frac{Z_P}{|\mathbf{R} - \mathbf{x}_{p i}|} \right| \varphi_p(\{\mathbf{x}_{p i}\}) \right\rangle, \quad (3)$$

which considers the interaction between the residual target and the projectile. In order to facilitate the calculations, the potentials ( $-Z_T/x + V_{ap}(\mathbf{x})$ ) are replaced by a coulombic one ( $-Z_T^*/x$ ), where an effective charge  $Z_T^*$  is chosen as  $Z_T^* = \sqrt{-2n_l^2 \varepsilon_i}$  [16], where  $n_l$  is the principal quantum number of the target electron orbital and  $\varepsilon_i$  is the corresponding active electron binding energy.

The initial wave function in a reference frame located on the target nucleus, both for ionization and capture, is chosen as

$$\begin{aligned} \chi_i^{ion, cap} &= \varphi_i(\mathbf{x}) \exp(-i\varepsilon_i t) \exp[-i\frac{Z_P}{v} \ln(\mathbf{v}\mathbf{s} + \mathbf{v}\mathbf{s})] \\ &\times \exp\{-i \int_{-\infty}^t V_S(\mathbf{R}) dt'\} = \\ &= \Phi_i^{ion, cap}(\mathbf{x}, t) \exp\{-i \int_{-\infty}^t V_S(\mathbf{R}) dt'\}, \end{aligned} \quad (4)$$

where  $\varphi_i(\mathbf{x})$  is the initial active electron bound state described within the Roothan-Hartree-Fock approximation [17].

The final wavefunction for ionization is chosen as

$$\begin{aligned} \chi_f^{ion} &= (2\pi)^{-3/2} \exp(-i\varepsilon_f^{ion} t + i\mathbf{k}\mathbf{x}) N^*(\xi)_1 \times F_1(-i\xi; 1; -ikx - i\mathbf{k}\mathbf{x}) \\ &\cdot N^*(\zeta)_1 F_1(-i\zeta; 1; -ipx - i\mathbf{p}\mathbf{x}) \times \exp\{i \int_t^{+\infty} V_S(\mathbf{R}) dt'\} \\ &= \Phi_f^{ion}(\mathbf{x}, t) \exp\{i \int_t^{+\infty} V_S(\mathbf{R}) dt'\}, \end{aligned} \quad (5)$$

where  $\mathbf{k}(\mathbf{p} = \mathbf{k} - \mathbf{v})$  is the linear momentum of the ejected electron with respect to the target (projectile) nucleus,  $\varepsilon_f^{ion} = k^2/2$  is the final electron energy,  $N(a) = \exp(\pi a/2) \Gamma(1 + ia)$  with  $\Gamma$  the Gamma function,  $\xi = Z_T^*/k$ ,  $\zeta = Z_P/p$  and  ${}_1F_1(a; 1; b)$  is the Coulomb continuum factor.

The final wavefunction for electron capture is taken as

$$\begin{aligned} \chi_f^{cap} &= \varphi_f(\mathbf{s}) \exp(-i\varepsilon_f^{cap} t + i\mathbf{v}\mathbf{x} - i\frac{v^2}{2} t) \cdot N^*(\beta)_1 F_1(-i\beta; 1; -ivx - i\mathbf{v}\mathbf{x}) \\ &\times \exp\{i \int_t^{+\infty} V_S(\mathbf{R}) dt'\} = \Phi_f^{cap}(\mathbf{s}, t) \exp\{i \int_t^{+\infty} V_S(\mathbf{R}) dt'\}, \end{aligned} \quad (6)$$

with  $\varphi_f(\mathbf{s})$  the final active electron bound state,  $\varepsilon_f^{cap}$  the corresponding orbital energy and  $\beta = Z_T^*/v$ . It has been demonstrated that with these choices of wavefunctions, radial electron correlation is included in the entry channel and the interaction between the passive and active electrons (dynamical screening) is considered in the exit one [18,19]. Hereby, the so-called two-center effect is taken into account in the 3B-CDW-EIS approximation.

Transition amplitudes

$$\begin{aligned} A_{if}^{ion, cap}(\boldsymbol{\rho}, \mathbf{k}) &= -i \int_{-\infty}^{+\infty} dt \langle \chi_f^{ion, cap} | H - i \frac{\partial}{\partial t} | \chi_i^{ion, cap} \rangle \\ &= -i \exp\{-i \int_{-\infty}^{+\infty} V_S(\mathbf{R}) dt\} \cdot \int_{-\infty}^{+\infty} dt \langle \Phi_f^{ion, cap} | H_e \\ &\quad - i \frac{\partial}{\partial t} | \Phi_i^{ion, cap} \rangle = a_{if}^{ion, cap} \exp\{-i \int_{-\infty}^{+\infty} V_S(\mathbf{R}) dt\} \end{aligned} \quad (7)$$

with

$$H_e = H - V_S(\mathbf{R}) \quad (8)$$

as a function of the impact parameter, both for ionization and capture, are analyzed.

We define the one-active electron ionization probability as,

$$\frac{d^3 P_{ion}(\boldsymbol{\rho}, \mathbf{k})}{dE_k d\Omega_k} = \frac{k}{2\pi} \int_0^{2\pi} d\varphi_\rho |a_{if}^{ion}(\boldsymbol{\rho}, \mathbf{k})|^2, \quad (9)$$

where  $E_k$  is the emitted electron energy and  $\Omega_k$  is the ejection angle.

Proceeding in a similar way, the impact-parameter-dependent single-particle probability for electron capture is given by,

$$P_{cap}(\boldsymbol{\rho}) = \frac{1}{2\pi} \int_0^{2\pi} d\varphi_\rho |a_{if}^{cap}(\boldsymbol{\rho})|^2, \quad (10)$$

where  $\varphi_\rho$  is the azimuthal angle of the impact parameter vector. It is clear that the interaction between the projectile and the residual target does not affect the ionization and capture probabilities defined by Eqs. (9) and (10). This behavior is supported by employment of the straight line version of the impact parameter approximation, which has been extensively used with success for both, ionization [12] and electron capture reactions [20]. Total cross sections (TCS) for SI and SC can be computed by means of,

$$\sigma_{SI, SC} = 2\pi \int \rho P_{tot}^{ion, cap}(\rho) d\rho, \quad (11)$$

where  $P_{tot}^{ion}$  is obtained after integration of Eq. (9) on  $E_k$  and  $\Omega_k$ . Total probabilities can be calculated using two different theoretical descriptions, 3B-CDW-EIS derived by Rivarola and co-workers, where SI and SC total probabilities are given by,

$$P_{tot}^{ion, cap}(\rho) = 2P_{ion, cap}(\rho), \quad (12)$$

and a second one, where a trinomial probability analysis is employed [21]. The TPA approximation was introduced to investigate the reaction of capture of  $m$  electrons and the ionization of  $l$  ones, so that the corresponding total probability is written as,

$$P_{m,l}(\rho) = \frac{N!}{m!l!(N-m-l)!} (P_{cap}(\rho))^m (P_{ion}(\rho))^l (1 - P_{ion}(\rho) - P_{cap}(\rho))^{N-m-l}, \quad (13)$$

where  $N$  is the total number of target electrons. For SI and SC Eq. (13) is reduced to

$$P_{TPA}^{ion, cap}(\rho) = 2P_{ion, cap}(\rho) \cdot (1 - P_{ion, cap}(\rho) - P_{cap, ion}(\rho)). \quad (14)$$

Considering that for transfer-ionization involving He atoms,  $N - m - l = 0$ , both models give the same TCS, so that one obtains,

$$P_{TI}(\rho) = 2P_{ion}(\rho) \cdot P_{cap}(\rho). \quad (15)$$

### 3. Results

Our interest is focused on the impact of  $\text{He}^{2+}$  and  $\text{Li}^{3+}$  ions on He targets. As we consider not only large impact energies but also intermediate ones for which electron capture may play a dominant role, this charge exchange reaction is also included in our analysis. We find that single-particle probabilities  $P_{ion}(\rho)$  and  $P_{cap}(\rho)$  can exceed unity at small impact parameters for low enough impact energies. Thus, in order to avoid these overestimations the unitarization procedure suggested by Sidorovich [22] is employed,

$$P_{\alpha}(\rho) = \frac{P_{\alpha}(\rho)}{[P_{ion}(\rho) + P_{cap}(\rho)]} \{1 - \exp[-(P_{ion}(\rho) + P_{cap}(\rho))]\}, \quad (16)$$

where the sub-index  $\alpha$  can be taken as *ion* or *cap*.

The corresponding results of SI total cross sections for the  $\text{He}^{2+}$  - He collision system are shown in Fig. 1 along with previous theoretical calculations and available experimental data. The 3B-CDW-EIS model provides better agreement with the experimental data [23–26] (giving in particular an adequate description of the experimental SI total cross section peak), than the TPA one, which largely underestimates the measurements. The final charge states of the projectile and target ions were measured in Refs [23–25]. In fact, in 3B-CDW-EIS it is assumed that to reduce the four-body reaction to a three-body one it is necessary to consider that the non-active electron remains frozen and bound to the residual target during the collision. Calculations employing a time-dependent density-functional-theory-basis-generator-method (TDDFT-BGM) [27] are also included in the figure. They are in close agreement with our 3B-CDW-EIS predictions except at impact energies smaller than approximately 150 keV/amu, where small differences are found.

Also close-coupling [28,29], classical trajectory Monte Carlo (CTMC) [29], non-equivalent electron (NEE) and equivalent electron (EE) approximations are depicted in Fig. 1. Close-coupling methods are in good agreement with the experimental data at high impact energies. Both CTMC results fail to reproduce the experiments.

SI total cross section results for the  $\text{Li}^{3+}$ -He collision system are presented in Fig. 2 along with previous models and available measurements. As for the  $\text{He}^{2+}$ -He collisions, the 3B-CDW-EIS model provides a very good description of experimental data

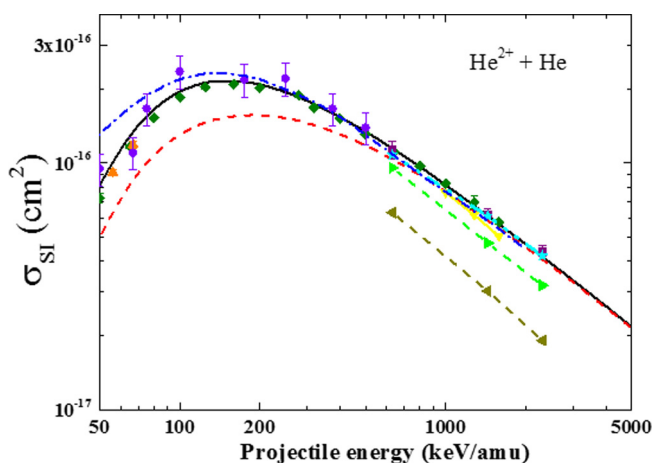


**Fig. 1.** SI cross sections in  $\text{He}^{2+}$ -He collisions. Theories: solid line, present results (3B-CDW-EIS with unitarization); dashed line, present results (TPA with unitarization); dash-dotted line, TDDFT-BGM [27]; solid line with filled downward triangles, Close-coupling [28]; dashed line with filled leftward triangles, NEE-CTMC [29]; dashed line with filled rightward triangles, EE-CTMC [29]; dash-dot-dotted line with filled stars, Coupled Channel [29]. Experiments: filled diamonds [23]; filled triangles [24]; filled circles [25]; filled squares [26].

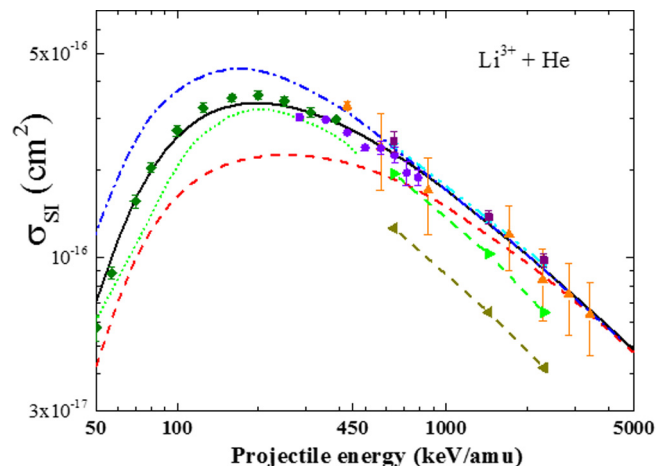


**Fig. 2.** SI cross sections in  $\text{Li}^{3+}$ -He collisions. Theories: solid line, present results (3B-CDW-EIS with unitarization); dashed line, present results (TPA with unitarization); dash-dotted line, CDW-EIS [12]; dotted line, Coupled Channel [32]; dashed line with filled leftward triangles, NEE-CTMC [29]; dashed line with filled rightward triangles, EE-CTMC [29]; dash-dot-dotted line with filled stars, Coupled Channel [29]. Experiments: filled diamonds [23]; filled triangles [30]; filled circles [31]; filled squares [26].

[23,26,30,31], where measurements were done in coincidence in Refs. [23,30,31]. The TPA model completely fails to describe the measured values. Again, 3B-CDW-EIS gives adequately the position of the experimental SI total cross section peak. The difference observed between the present one-electron model and the CDW-EIS one [12], also shown in Fig. 2, is due to applying a post-version of the CDW-EIS approximation without unitarization procedure. However, we must remark that transition probabilities can be larger than one.

In Fig. 2, coupled-channel [29,32], NEE-CTMC and EE-CTMC [29] calculations are also presented. The coupled-channel method of Ref. [32] shows correctly the general trend of the experiments although they are underestimated. On the contrary, the coupled-channel method of Ref. [29] describes well experimental data at high impact energies. Both CTMC results fail to reproduce the experiments.

SC total cross sections are displayed in Fig. 3 along with a set of theories and available experimental results for the  $\text{He}^{2+}$  - He

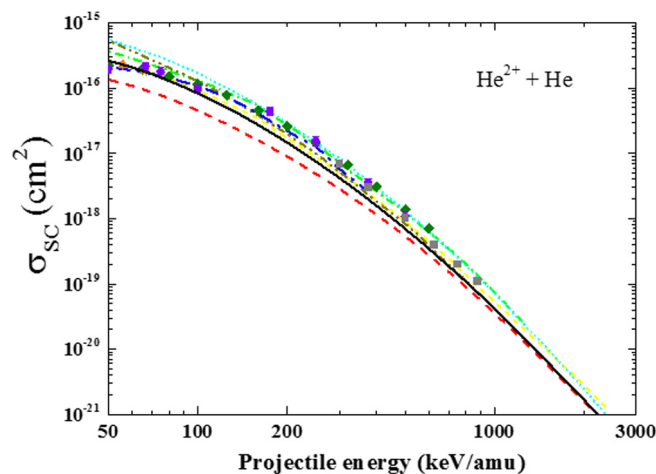


**Fig. 3.** SC cross sections in  $\text{He}^{2+}$ -He collisions. Theories: solid line, present results (3B-CDW-EIS with unitarization); dashed line, present results (TPA with unitarization); short-dash-dotted line, BCCIS-4B [34]; short-dashed line, DW-4B [35]; dotted line, CB1-4B [36]; dash-dot-dotted line, BDW-3B [37]; dash-dotted line, TDDFT-BGM [27]. Experiments: filled diamonds [23]; filled triangles [24]; filled circles [25]; filled squares [33].

collision system. 3B-CDW-EIS provides better agreement with experimental data [23–25,33], where measurements were done in coincidence in Refs. [23–25], than TPA. Previous BCCIS-4B (four-body boundary-corrected continuum-intermediate-state) [34], DW-4B (four-body distorted wave) [35], CB1-4B (four-body boundary-corrected first Born) [36], BDW-3B (three-body Born distorted wave) [37] and TDDFT-BGM [27] calculations are depicted in Fig. 3. All results show adequate agreement with the experimental data. On the contrary, TPA largely underestimates the experiments. However, we should mention that present 3B-CDW-EIS also gives a small underestimation of the measurements for impact energies larger than 100 keV/amu. One possible reason for this behavior could be attributed to the fact that for these impact velocities ionization probabilities are much larger than electron capture ones and may act as an intermediate mechanism contributing to the charge-exchange process. This influence is not considered in our model. Also intermediate excitation channels could give some contribution to SC.

Our SC total cross sections results for the  $\text{Li}^{3+}$ -He collision system are shown in Fig. 4. It is seen that 3B-CDW-EIS, giving the general trend but underestimating the measurements, again provides better agreement with the experimental data [23,30,31] than the TPA model. The reasons for this underestimation are similar to the arguments given for  $\text{He}^{2+}$  projectile. Previous BCCIS-4B [34], DW-4B [35], CB1-4B [36] and BDW-3B [37] calculations are depicted in Fig. 4. The results of Refs. [34–36] are in good agreement with measurements, but the model of Ref. [36] starts to overestimate experiments at intermediate to low projectile impact energies. 3B-CDW-EIS gives almost the same shape of the SC total cross section as the one of the model of Ref. [37].

Next, we will discuss our results regarding transfer-ionization for the  $\text{He}^{2+}$ -He collision system, which are displayed in Fig. 5. It is seen that the 3B-CDW-EIS model is in very good agreement with the experimental data [23–25]. Previous CDW-4B (four-body Continuum Distorted Wave) [38], Born 2 [39] and TDDFT-BGM [27] calculations are presented in Fig. 5. The model of Ref. [38] overestimates the measurements at high and low impact energies, whereas it underestimates them at the intermediate range. The model of Ref. [39] slightly underestimates the experiments and the model of Ref. [27] describes the experimental data at low impact energies and underestimates or overestimates them at intermediate to high impact energies range, respectively.

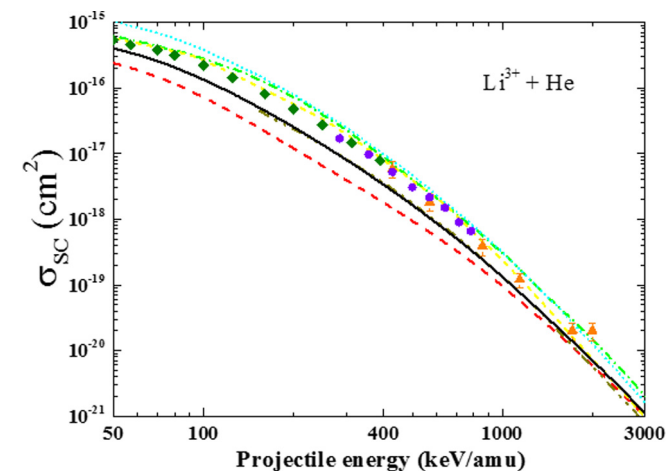


**Fig. 4.** SC cross sections in  $\text{Li}^{3+}$ -He collisions. Theories: solid line, present results (3B-CDW-EIS with unitarization); dashed line, present results (TPA with unitarization); short-dash-dotted line, BCCIS-4B [34]; short-dashed line, DW-4B [35]; dotted line, CB1-4B [36]; dash-dot-dotted line, BDW-3B [37]. Experiments: filled diamonds [23]; filled triangles [30]; filled circles [31].

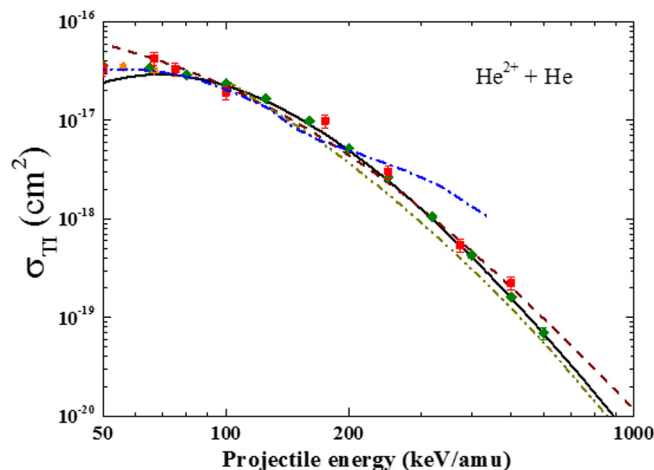


**Fig. 5.** TI cross sections in  $\text{He}^{2+}$ -He collisions. Theories: solid line, present results (3B-CDW-EIS with unitarization); dashed line, CDW-4B [38]; dash-dot-dotted line, Born 2 [39]; dash-dotted line, TDDFT-BGM [27]. Experiments: filled diamonds [23]; filled triangles [24]; filled circles [25].

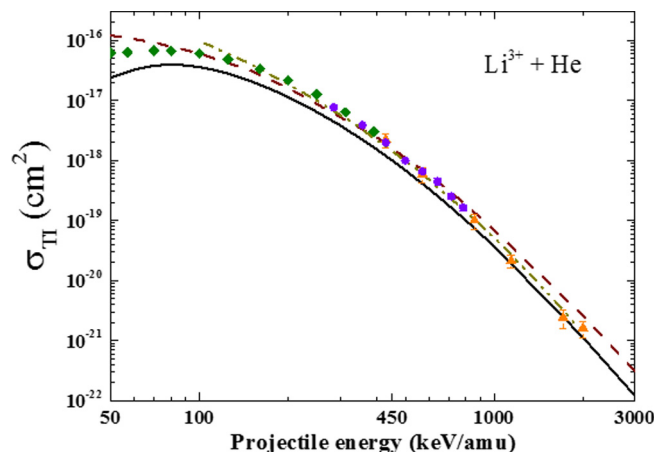


**Fig. 6.** TI cross sections in  $\text{Li}^{3+}$ -He collisions. Theories: solid line, present results (3B-CDW-EIS with unitarization); dashed line, CDW-4B [40]; dash-dot-dotted line, Born 2 [39]. Experiments: filled diamonds [23]; filled triangles [30]; filled circles [31].

TI total cross sections for the  $\text{Li}^{3+}$ -He collision system are plotted in Fig. 6. We can conclude that the 3B-CDW-EIS model is in good agreement with measurements [23,30,31] at high impact energies and underestimates them at intermediate to low ones. As it was mentioned for SC process, the reason could be attributed to the influence of ionization and excitation intermediate channels. Previous CDW-4B [40] and Born 2 [39] calculations are presented in Fig. 6. Both results show an adequate description of the experiments.

#### 4. Conclusions

We have investigated single electron ionization, single electron capture and transfer-ionization processes of helium targets impacted by  $\text{He}^{2+}$  and  $\text{Li}^{3+}$  projectiles at intermediate and high collision energies. Single particle probabilities for ionization and capture were obtained as a function of the impact parameter in the framework of the 3B-CDW-EIS model. The procedure proposed by Sidorovich [22] was employed to obtain unitarized ionization and capture probabilities. 3B-CDW-EIS shows better agreement



with the experimental data for both considered projectiles than the trinomial probability description. The success of 3B-CDW-EIS to describe SI and SC could be attributed to the fact that in this model the non-active electron is assumed to be frozen in its initial orbital. This means that the passive electron cannot be captured nor ionized. However, for SC it appears that ionization and excitation intermediate states could play some role. The relatively good agreement between theory and experiments for single processes in the case of  $\text{He}^{2+}$  ions encouraged us to tackle with more complex multiple reactions, as transfer-ionization. For the higher charged  $\text{Li}^{3+}$  projectile, 3B-CDW-EIS gives the general trend of measurements but underestimate them. This behavior could come from the underestimation of SC total cross section. However, one must remark that the agreement between 3B-CDW-EIS calculations and experiments is very good at high impact energies for all the studied reactions.

The use of a trinomial probability description completely fails to adequately represent SI and SC processes for these small multielectronic targets. On the other side, we should mention that a multinomial probability analysis relies on the assumption that they are calculated for single processes and fully independent (uncorrelated) one of the other. This lack of independency appears as crucial for these light targets.

The developed approach for calculation of one-electron ionization and capture probabilities allows to investigate multiple electron processes for complex targets in particular such as macromolecules of DNA and RNA to model scenarios for the radiobiological consequences of the impact of charged energetic particles on those macromolecules.

### Acknowledgements

Authors acknowledge financial support from the Agencia Nacional de Promoción Científica y Tecnológica (PICT 2011-2012) and the Consejo Nacional de Investigaciones Científicas y Técnicas de la República Argentina (PIP No. 11220090101026). The simulations were performed on resources of the Computer Cluster of the Institute of Physics Rosario. P.N. Terekhin thanks K.V. Vodopyanov for providing additional computing power.

### References

- [1] T.E. Cravens, *Science* 296 (2002) 1042.
- [2] S.Yu Simon et al., *Nucl. Fusion* 47 (2007) 721.
- [3] I. Murakami, J. Yan, H. Sato, M. Kimura, R.K. Janev, T. Kato, *At. Data Nucl. Data Tables* 94 (2008) 161.

- [4] J. Ullrich, R. Moshhammer, A. Dorn, R. Dörner, L.Ph.H. Schmidt, H. Schmidt-Böcking, *Rep. Prog. Phys.* 66 (2003) 1463.
- [5] R.D. Rivarola, R.D. Piacentini, A. Salin and Dž. Belkić, *J. Phys. B: At. Mol. Opt. Phys.* 13 (1980) 2601.
- [6] P.D. Fainstein, V.H. Ponce, R.D. Rivarola, *J. Phys. B: At. Mol. Opt. Phys.* 21 (1988) 287.
- [7] J.H. McGuire, *Electron Correlation Dynamics in Atomic Collisions*, Cambridge University Press, Cambridge, 1997, p. 85.
- [8] M.M. Sant'Anna, E.C. Montenegro, J.H. McGuire, *Phys. Rev. A* 58 (1998) 2148.
- [9] M.E. Galassi, R.D. Rivarola, P.D. Fainstein, *Phys. Rev. A* 75 (2007) 052708.
- [10] L. Gulyás, S. Egri, H. Ghavamnia, A. Igarashi, *Phys. Rev. A* 93 (2016) 032704.
- [11] T. Kirchner, L. Gulyás, R. Moshhammer, M. Schulz, J. Ullrich, *Phys. Rev. A* 65 (2002) 042727.
- [12] P.D. Fainstein, V.H. Ponce, R.D. Rivarola, *J. Phys. B: At. Mol. Opt. Phys.* 24 (1991) 3091.
- [13] A.E. Martínez, G.R. Deco, R.D. Rivarola, P.D. Fainstein, *Nucl. Instrum. Methods Phys. Res., Sect. B* 34 (1988) 32.
- [14] H.F. Busnengo, A.E. Martínez, R.D. Rivarola, L.J. Dubé, *J. Phys. B: At. Mol. Opt. Phys.* 28 (1995) 3283.
- [15] D.S.F. Crothers, J.F. McCann, *J. Phys. B: At. Mol. Opt. Phys.* 16 (1983) 3229.
- [16] Dž. Belkić, R. Gayet, A. Salin, *Phys. Rep.* 56 (1979) 279.
- [17] E. Clementi, C. Roetti, *At. Data Nucl. Data Tables* 14 (1974) 177.
- [18] J.M. Monti, O.A. Fojón, J. Hanssen, R.D. Rivarola, *J. Phys. B: At. Mol. Opt. Phys.* 43 (2010) 205203.
- [19] J.M. Monti, O.A. Fojón, J. Hanssen, R.D. Rivarola, *J. Phys. B: At. Mol. Opt. Phys.* 46 (2013) 145201.
- [20] S.E. Corchis, R.D. Rivarola, J.H. McGuire, *Phys. Rev. A* 47 (1993) 3937, and references therein.
- [21] M. Horbatsch, *Phys. Lett. A* 187 (1994) 185.
- [22] V.A. Sidorovich, V.S. Nikolaev, *J. Phys. B: At. Mol. Opt. Phys.* 16 (1983) 3243.
- [23] M.B. Shah, H.B. Gilbody, *J. Phys. B: At. Mol. Opt. Phys.* 18 (1985) 899.
- [24] M.B. Shah, P. McCallion, H.B. Gilbody, *J. Phys. B: At. Mol. Opt. Phys.* 22 (1989) 3037.
- [25] R.D. DuBois, S.T. Manson, *Phys. Rev. A* 36 (1987) 2585.
- [26] H. Knudsen, L.H. Andersen, P. Hvelplund, G. Astner, H. Cederquist, H. Danared, L. Liljeby, K.-G. Rensfelt, *J. Phys. B: At. Mol. Opt. Phys.* 17 (1984) 3545.
- [27] M. Baxter, T. Kirchner, *Phys. Rev. A* 93 (2016) 012502.
- [28] M.S. Pindzola, F. Robicheaux, J. Colgan, *J. Phys. B: At. Mol. Opt. Phys.* 40 (2007) 1695.
- [29] I.F. Barna, K. Tökési, J. Burgdörfer, *J. Phys. B: At. Mol. Opt. Phys.* 38 (2005) 1001.
- [30] O. Woiatke, P.A. Závodszky, S.M. Ferguson, J.H. Houck, J.A. Tanis, *Phys. Rev. A* 57 (1998) 2692.
- [31] M.M. Sant'Anna, A.C.F. Santos, L.F.S. Coelho, G. Jalbert, N.V. de Castro Faria, F. Zappa, P. Focke, Dž. Belkić, *Phys. Rev. A* 80 (2009) 042707.
- [32] R. Shingal, C.D. Lin, *J. Phys. B: At. Mol. Opt. Phys.* 24 (1991) 251.
- [33] N.V. de Castro Faria, F.L. Freire Jr., A.G. de Pinho, *Phys. Rev. A* 37 (1988) 280.
- [34] R. Samanta, M. Purkait, C.R. Mandal, *Phys. Rev. A* 83 (2011) 032706.
- [35] S. Jana, C.R. Mandal, M. Purkait, *J. Phys. B: At. Mol. Opt. Phys.* 48 (2015) 045203.
- [36] I. Mančev, N. Milojević, Dž. Belkić, *At. Data Nucl. Data Tables* 102 (2015) 6.
- [37] M. Rahmianian, F. Shojaei, R. Fathi, *J. Phys. B: At. Mol. Opt. Phys.* 49 (2016) 175201.
- [38] Dž. Belkić, R. Gayet, J. Hanssen, I. Mančev, A. Nuñez, *Phys. Rev. A* 56 (1997) 3675.
- [39] A.L. Godunov, J.H. McGuire, V.S. Schipakov, H.R.J. Walters, Colm T. Whelan, *J. Phys. B: At. Mol. Opt. Phys.* 39 (2006) 987.
- [40] I. Mančev, *Phys. Rev. A* 64 (2001) 012708.